SUPPLEMENTARY MATERIAL for

Structural sensitivity of a prokaryotic pentameric ligand-gated ion channel to its membrane environment*

Jonathan M. Labriola[1], Akash Pandhare[2], Michaela Jansen[3], Michael P. Blanton[2], Pierre-Jean Corringer[4], and John E. Baenziger[1]

[1]From the Department of Biochemistry, Microbiology, and Immunology
University of Ottawa, Ottawa ON, K1H 8M5, Canada

[2]Department of Pharmacology and Neuroscience and the Center for Membrane Protein Research, School of Medicine, Texas Tech University Health Sciences Center, Lubbock, TX 79430

[3]Department of Cell Physiology and Molecular Biophysics and the Center for Membrane Protein Research, School of Medicine, Texas Tech University Health Sciences Center, Lubbock, TX. 79430.

[4]G5 Group of Channel-Receptors, CNRS URA 2182
Pasteur Institute, F75015, Paris, France

*Running title: *Lipid sensitivity of a prokaryotic pLGIC*

[1]To whom correspondence should be addressed: John E. Baenziger, Department of Biochemistry, Microbiology, and Immunology, University of Ottawa, 451 Smyth Rd. Ottawa, ON, K1H 8M5, Canada, Tel.: (613) 562-5800 x8222; Fax.: (613) 562-5440; E-mail: John.Baenziger@uottawa.ca.

Includes: Supplemental Figures S1-S6 with captions

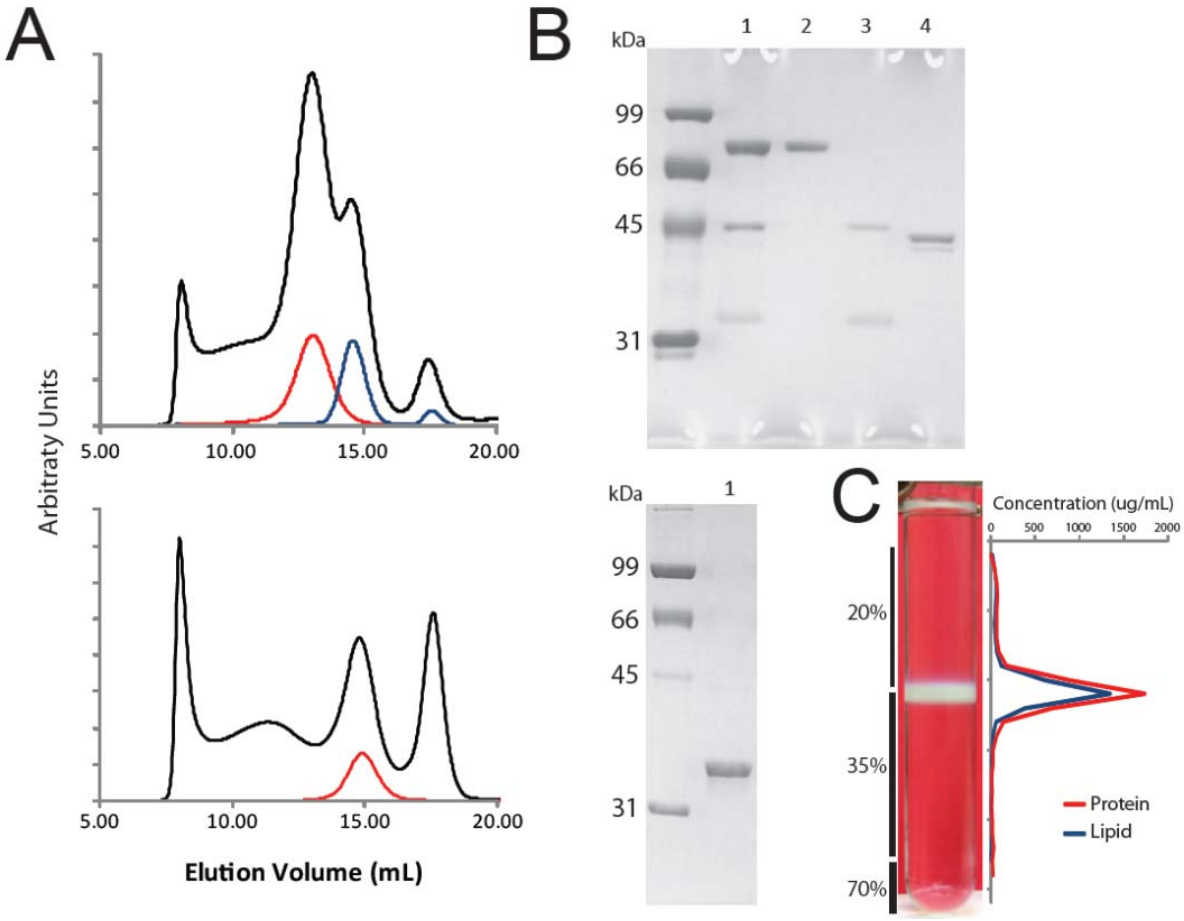

Figure S1. Purification and reconstitution of GLIC. (A) The elution profiles of MBP-GLIC (top set of traces) or GLIC (bottom traces) from an SEC column. In both cases, MBP-GLIC was affinity purified on an amylose affinity resin. The MBP-GLIC was eluted using maltose, while GLIC was eluted after cleavage of the MBP-GLIC linker with thrombin. The affinity purified proteins were concentrated and then passed through the SEC column leading to the elution profiles shown in black. In the top set of traces, the red trace ~13 mls corresponds to purified MBP-GLIC, the purple trace at ~15 mls corresponds to an endogenous *E. coli* protein that binds to the amylose resin, and the purple trace at ~17 mls corresponds to MBP. In the bottom set of traces, the red trace at ~15 mls corresponds to purified GLIC. Individual traces are arbitrarily scaled for presentation purposes. (B) SDS PAGE gels of the eluted fractions from the SEC. Top gel *Lane 1*, concentrated MBP-GLIC plus endogenous *E. coli* protein eluted from the amylose affinity resin; *Lane* 2, MBP-GLIC; *Lane 3*, unknown *E. coli* protein; *Lane 4*, MBP. Bottom gel *Lane 1*, purified GLIC. (C) Sucrose density gradient purification of reconstituted aso-GLIC showing complete incorporation of GLIC into the asolectin membranes. The lipid assay measures choline content, and thus underestimates the lipid content of the reconstituted membranes.

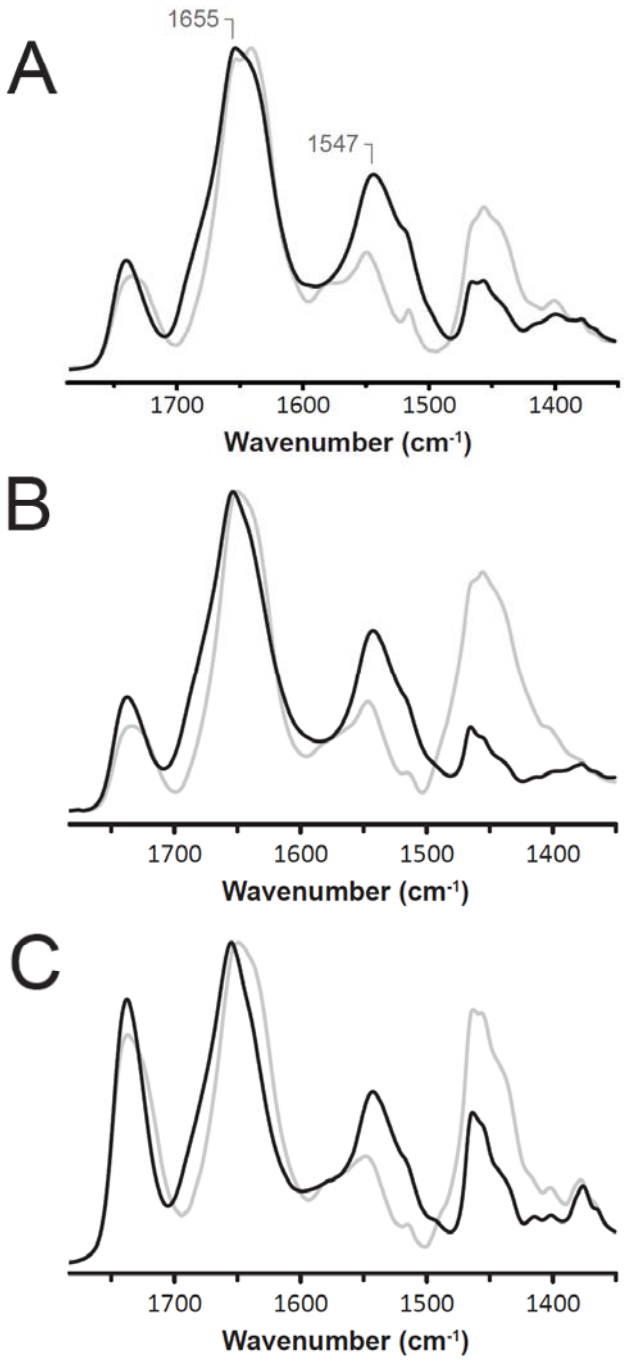

Figure S2. Infrared spectra recorded from (A) GLIC, (B) the nAChR, and (C) the α4β2 neuronal nAChR recorded after gentle drying to remove bulk solvent from $^{1}H_2O$ buffer (solid black line) and immediately after addition of $^{2}H_2O$ (dashed grey line). Note the immediate changes in amide I band shape (1700 – 1600 cm^{-1}) and the immediate decrease in amide II band intensity (1547 cm^{-1}), both indicative of the rapid peptide N-^{1}H/N-^{2}H exchange of solvent exposed regions of the polypeptide backbone. (data from daCosta et al. (2011) *Biochem Biophy. Res Commun* **407**, 456-460)

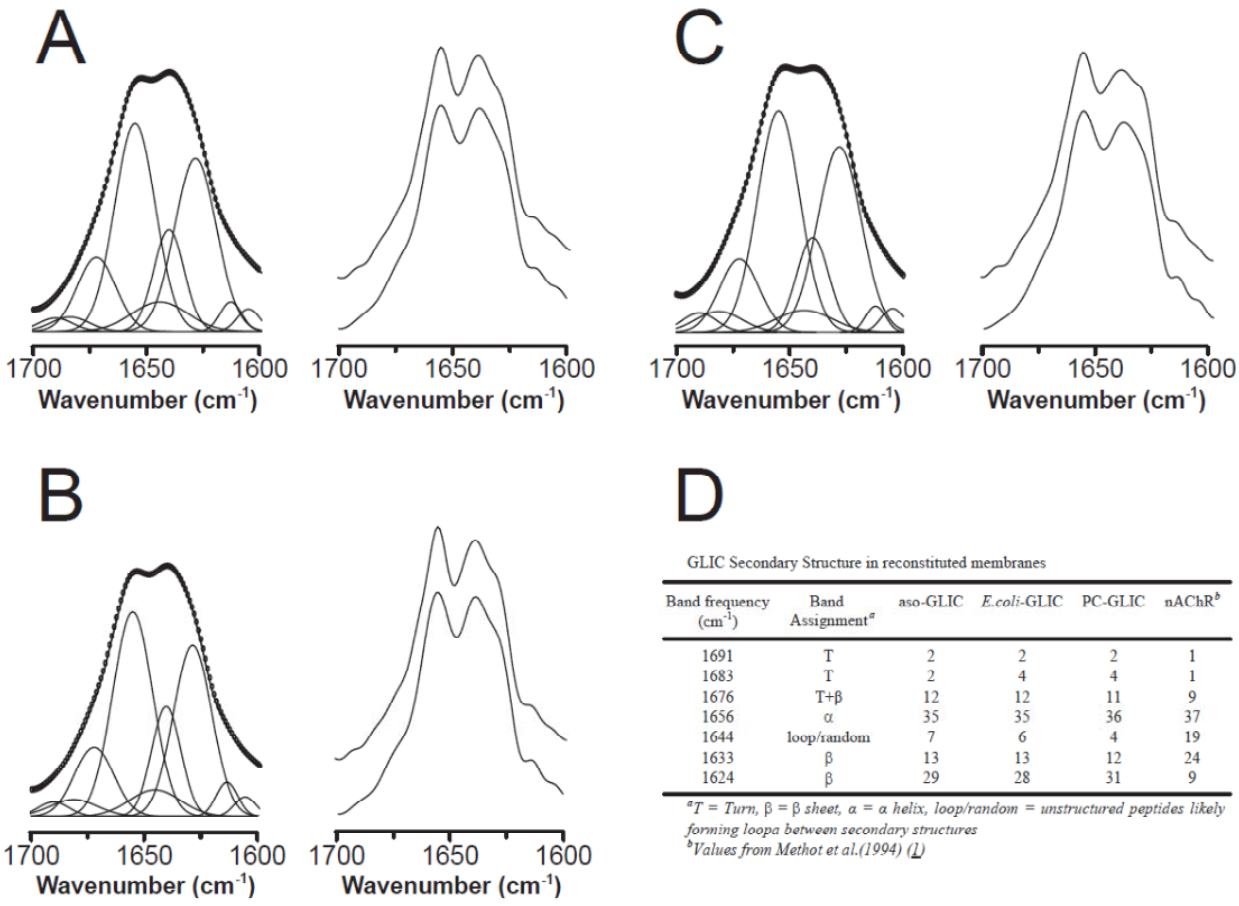

D

GLIC Secondary Structure in reconstituted membranes

Band frequency (cm^{-1})	Band Assignment[a]	aso-GLIC	*E.coli*-GLIC	PC-GLIC	nAChR[b]
1691	T	2	2	2	1
1683	T	2	4	4	1
1676	T+β	12	12	11	9
1656	α	35	35	36	37
1644	loop/random	7	6	4	19
1633	β	13	13	12	24
1624	β	29	28	31	9

[a]T = Turn, β = β sheet, α = α helix, loop/random = unstructured peptides likely forming loops between secondary structures

[b]Values from Methot et al.(1994) (1)

Figure S3. Representative curve fits of the amide I bands from (A) aso-GLIC, (B) EcoLip-GLIC, and (C) PC-GLIC. In each case, the left set of spectra include the experimental amide I absorbance contour (black line), the superimposed curve fit (open circles), and the individual component peaks summed to curve fit amide I contour. The two spectra on the right correspond to the the deconvolved experimental spectrum (top) and the deconvolved curve fit spectrum (bottom). (D) The resulting curve fit estimates and band assignments.

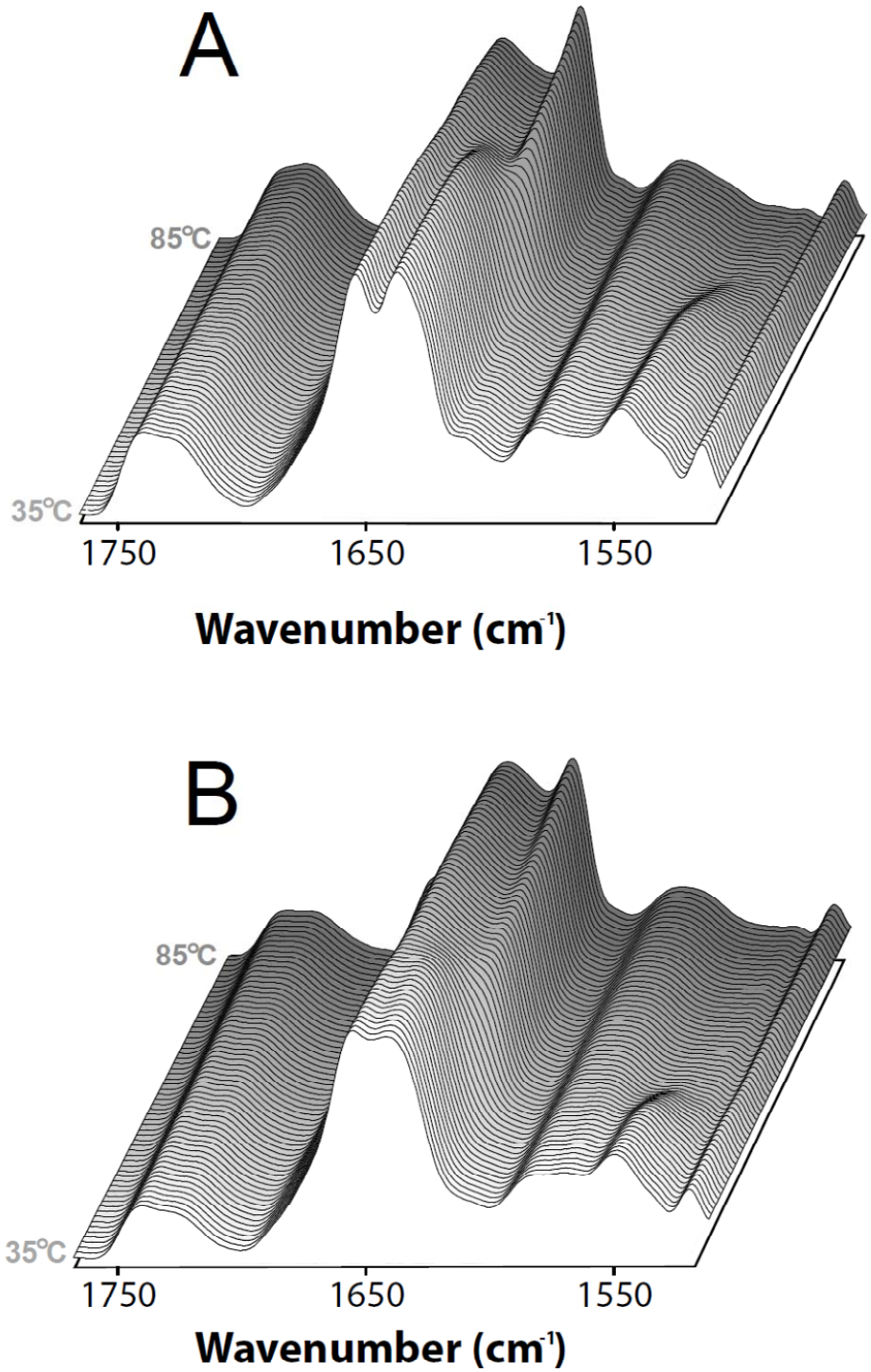

Figure S4. Stacked plot of spectra collected for thermal stability characterization of (A) aso-GLIC and (B) aso-nAChR. Representative traces are shown from 35 °C to 85 °C, front to back. Spectra were collected at 1˚C increments.

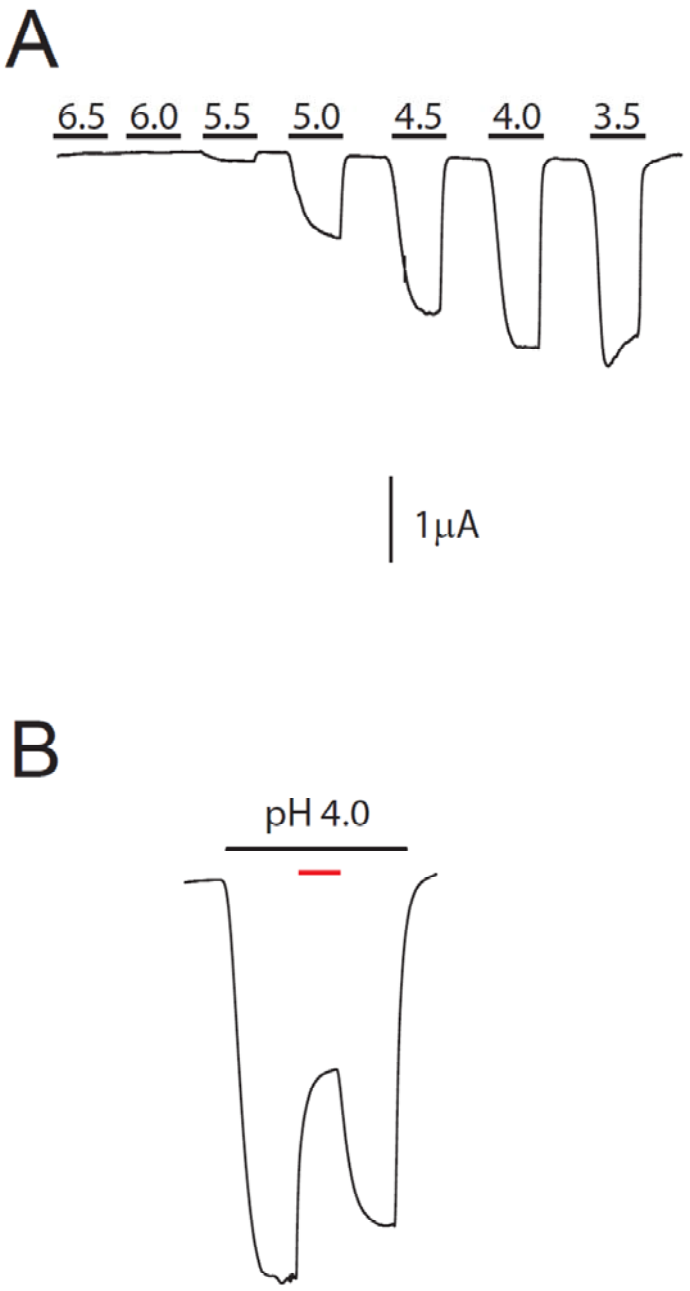

Figure S5. Current traces of mRNA-GLIC injected oocyted probed by two-electrode voltage clamp. (A) Currents induced by exposure to the pH jumps indicated by the horizontal bars. Cells were held at a membrane potential of -20 mV. (B) mRNA-GLIC injected oocytes were held at a membrane potential of -60mV and exposed to pH 4.0 until steady state was achieved, after which 150μM amantadine (pH 4.0) was introduced into cell profusion chamber (red bar) followed by washout.

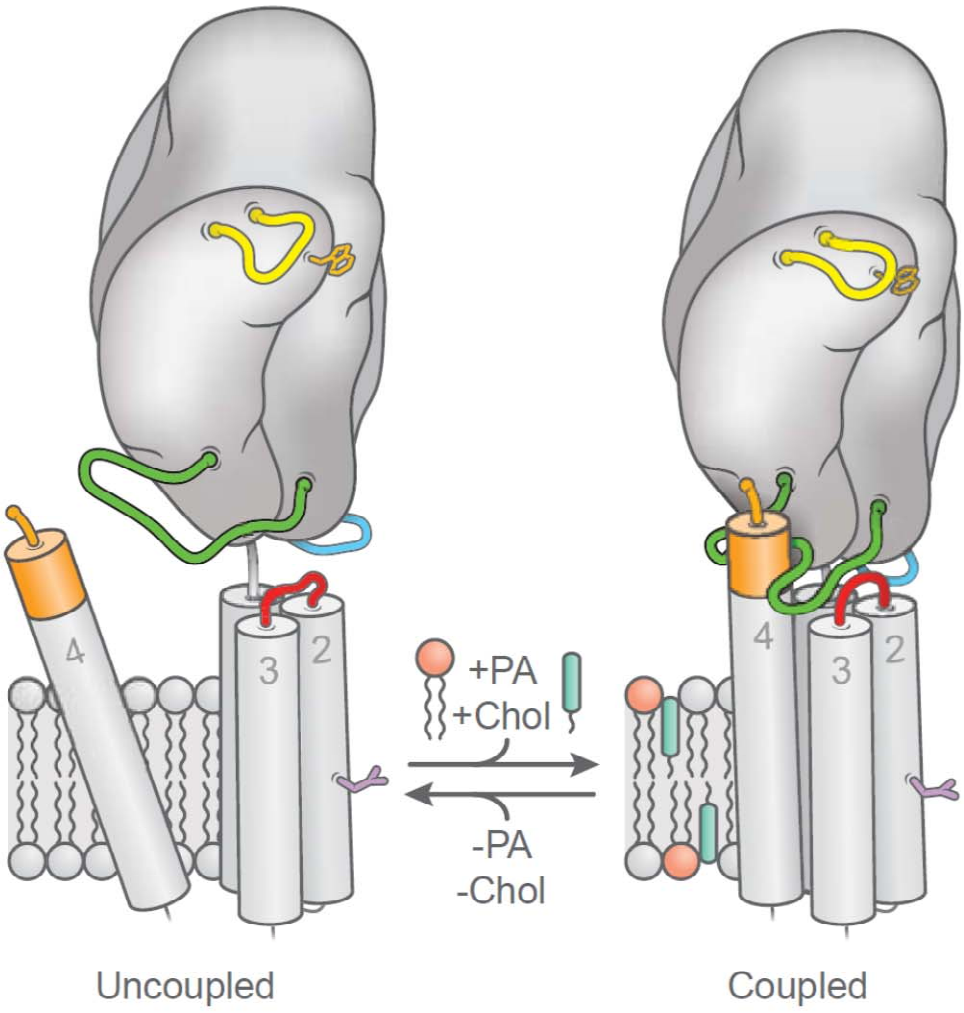

Figure S6. The M4 lipid-sensor model of uncoupling. The model proposes that interactions between the C-terminus of M4 (orange) forms critical interactions with the Cys-loop (green) of the agonist binding domain. When optimal interactions occur, the Cys-loop adopts a conformation that allows tight interactions with the M2-M3 linker. These tight interactions are essential for coupling binding to gating. In unfavorable lipid environments, the interactions between M4 and the Cys-loop are not optimatal. This leads to an altered conformation of the Cys-loop and weakened interactions between the Cys-loop and M2-M3 linker. Weakened interactions leads to a physical separation between the agonist-binding and transmembrane domains and thus the uncoupling of binding and gating. (daCosta & Baenziger (2009) *J Biol Chem* **284**, 17819-17825)